URTeC: 2690022

Monitoring Hydraulic Fracturing Fluid Movement using Ground-Based Electromagnetics, with Applications to the Anadarko Basin and the Delaware Basin / NW Shelf

Mark S. Hickey*, Santiago Treviño III, Deep Imaging Technologies Inc.; Mark E. Everett, Texas A&M University.

This paper was prepared for presentation at the Unconventional Resources Technology Conference held in Austin, Texas, USA, 24-26 July 2017.

Abstract

Hydraulic fracturing provides the petroleum industry with unconventional means for extracting hydrocarbons, but the method can be made more efficient to enable better production by answering some not so simple questions: where did the injection fluid go and how much of the volume was propped? Ground-based controlled source electromagnetics (CSEM) provides a means to generate, record, and interpret electromagnetic signals responding to temporal changes in the subsurface electrical conductivity, using instruments deployed on the surface. Since the injection of fluid into rock for hydraulic fracturing alters the conductivity of the formation in the vicinity of the wellbore, CSEM is a geophysical technique that is well-suited for monitoring completions. In this paper we show results from two CSEM surveys. The first CSEM survey acquired data from the Anadarko basin during hydraulic fracture operations from a lateral well while the second CSEM survey is based on data obtained during the completions of a vertical well in the Delaware basin/ Northwest shelf. Both of the surveys provided unique challenges. The data interpretations from each survey help to influence future completion strategies by providing valuable information to the well development teams, for example fracture asymmetry, fracture half lengths, and unexpected fracture behavior.

Introduction

Ground-based controlled-source electromagnetics (CSEM) is an emerging geophysical technique that can be used to monitor the movement and extent of injection fluid during hydraulic fracture operations (1,2). The electromagnetic response of a conductive zone containing fluid to its energization by a surface-deployed CSEM source is dependent upon the electrical conductivity difference between the fluid-rich zone and the background geological formation (3). The fact that CSEM is sensitive to the electrical conductivity of the fluid allows properties such as hydraulic fracture half-length and fracture asymmetry to be studied dynamically. Additionally, it has been shown that the presence of a steel well casing increases the sensitivity to deep targets (4,5). We now present two case studies, the first involving a horizontal well in the Anadarko Basin and the second involving a vertical well in the Delaware basin Northwest shelf.

Modeling

In order to characterize the expected CSEM response of an anomalously conductive target we use 3-D CSEM finite-element forward modeling (1,2,3). The governing Maxwell's equations are solved in the frequency domain for the response of a secondary set of EM potentials ($\mathbf{A}_s$,Ψ_s) with conductivity structure $\sigma_s(\mathbf{r})$, herein representing zones containing frac fluid, by first specifying a set of known electromagnetic (EM) primary potentials ($\mathbf{A}_p$, Ψ_p) as the response to a background conductivity structure $\sigma_p(\mathbf{r})$, i.e. the response produced by the interaction of the transmitted signal with the underlying geologic structure. Analysis of the expected "secondary" response in the presence of the frac fluid aids in survey layout design and interpretation. As an example, consider a modeling domain of dimensions 17.2 km× 17.2 km × 19 km. The model comprises a half-space background conductivity of 0.01 S/m and a conductive target at depth 3080 m with a width of 140 m in the x-direction, 280 m in the y-direction and thickness of 35 m. A 60 A, 600 m long x-directed horizontal dipole is placed at the surface (z = 0.0 m) and centered at the origin. For a receiver also on the surface located at x =140 m and y = 140 m, Figure 1 shows how the magnitude of the x-component of the Electric field changes as target conductivity (measured in S/m) changes. Additionally, it can be shown that the frequency at which the Electric field amplitude attains its maximum shifts with target depth.

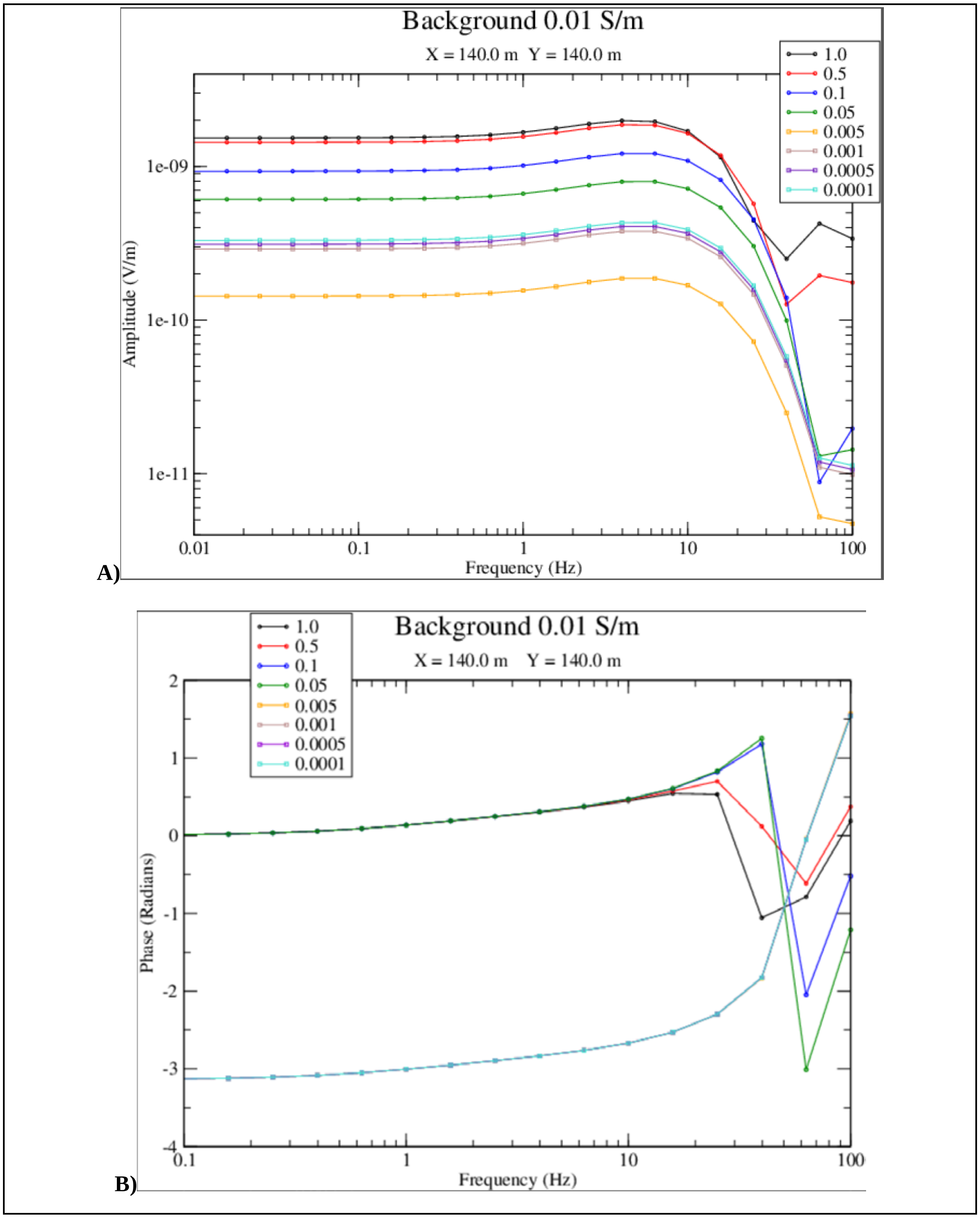

Figure 1: Frequency response of A) the amplitude B) the phase of the x-component of the Electric field as target conductivity [S/m] changes.

Field Methodology and Data Processing

A typical layout of the receiver array and the grounded-dipole transmitter for hydraulic fracture monitoring is displayed in Figures 2A and 2B. The transmitter dipole of length 600 m runs parallel to, and lies on the surface directly above, the lateral well. Figure 2B is a close-up of a portion of the layout that shows the electric-dipole receivers, including their electrode pairs and control boxes. Receivers are placed on each side of the lateral with the

Figure 2: Anadarko Basin Layout A) Receivers are placed symetrically on each side of the transmitter line. B) A zoomed in version to show the perpendicular and parallel components.

receiver electrode pairs arranged parallel and perpendicular to the transmitter line. Each receiver is able to record on multiple channels simultaneously, with the recorded signal from each receiver electrode-pair being treated as a separate datum. Receiver electrode separation distances are typically 30 m.

After electric-field data are collected from a receiver, the dataset is processed, transformed into the frequency domain, and then subtracted from the background, pre-frac response. This results in a signal that represents the response due to the fluid injection, assuming that no other changes to subsurface electrical conductivity or systematic variations of the background electromagnetic environment are present. Depending on the amount of fluid being injected and the depth of injection, the amplitude of the response is enhanced over a certain frequency range. The amplitudes from a selected frequency range are summed and the resulting aggregate signal is displayed in plan view for interpretation. A threshold for noise is determined based on the number of frequencies summed and the background noise at the site location. A signal is considered significant if its peak strength is about 2 orders of magnitude larger than the background pre-frac signal at the same location.

Case Study 1: Anadarko Basin

For the first case study, CSEM data were acquired directly above the toe end of a horizontal wellbore in the Anadarko Basin. In this case the standard layout shown in Figure 2 was used. The results from stage-2 operations, which was the first stage electromagnetically monitored, are presented as contour maps in Figures 3A and 3B. Figure 3A shows the initial response at the beginning of the fracture operation. Note that each datum displayed is the aggregate response, summed over a selected frequency range, of the transmitter-parallel component of the electric field recorded at the receiver location. The response shown in the areas between receivers is the value interpolated from responses measured at nearby receivers. Initially the largest response appears to the NW of the stage location. Figure 3B shows the fracture-related CSEM response at the final time step, i.e. at the end of the stage operation, where the largest response appears to the SE. From these Stage-2 CSEM results, the half-length of the hydraulic fracture can be estimated and, although in this case the largest hydraulic fracture-induced CSEM signals appear on different sides of the well at different times, the azimuth of a line joining them provides important information about the geometry of the fluid injection pathways. The general area and direction of the fracture signals are represented by ellipses and arrows to enable a comparison with CSEM responses measured during later stages.

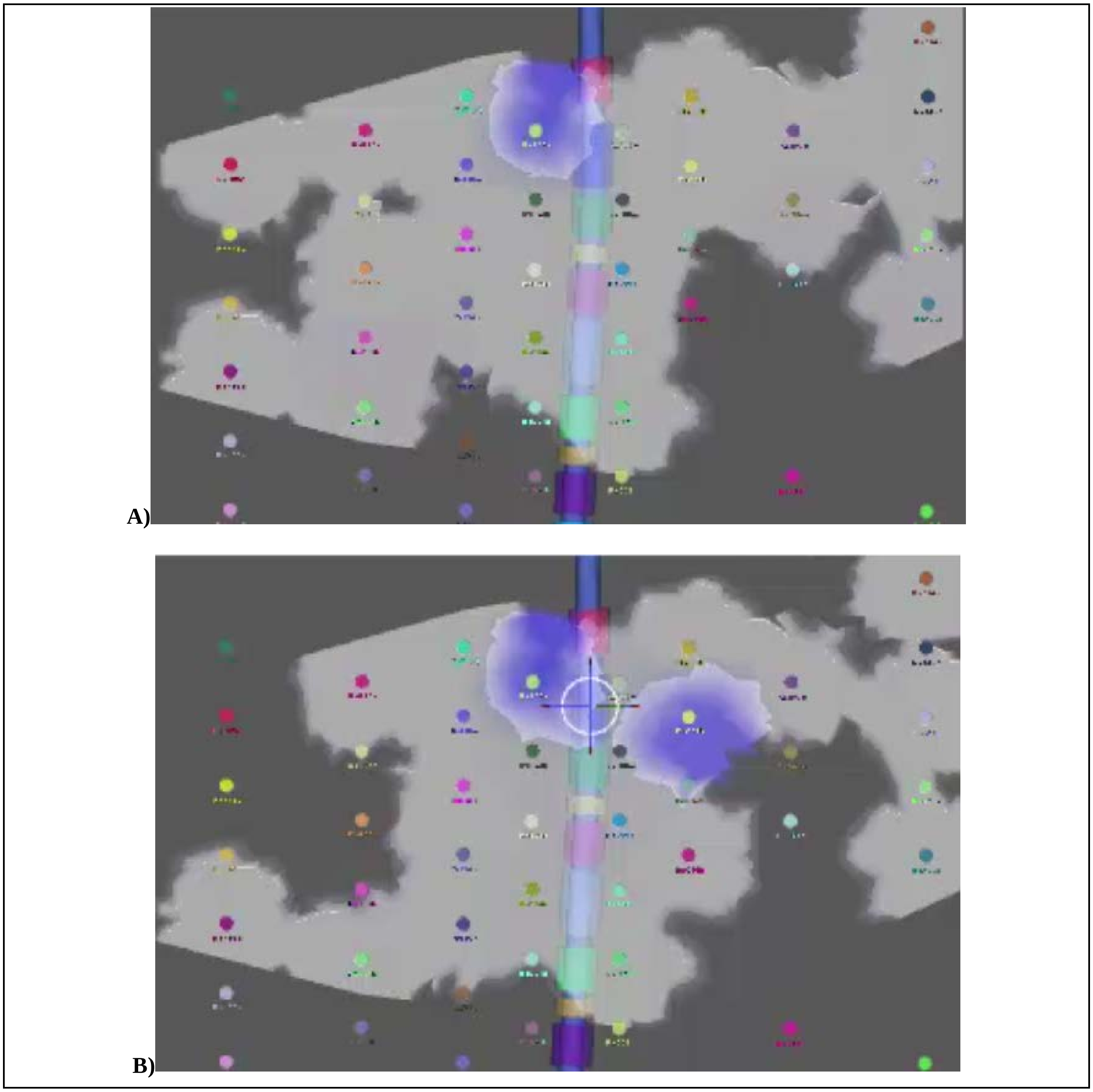

Figure 3: Stage 2 displaying the A) Initial frac signal B) Final frac signal.

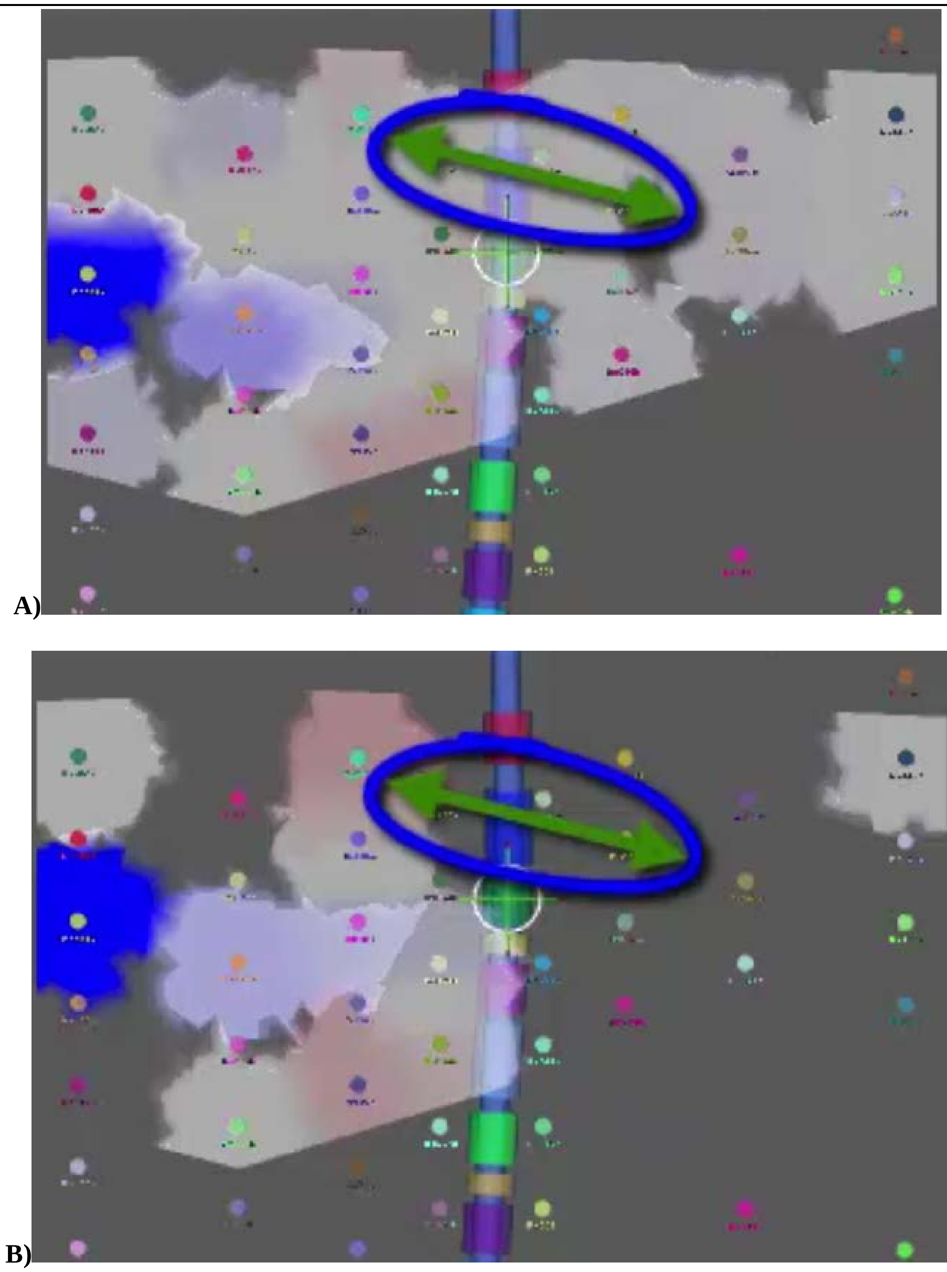

Figure 4: Stage 3 displaying the A) Initial frac signal B) Final frac signal.

The CSEM responses from the stage-3 operations are shown in Figures 4A and 4B. In this case, the initial signal shown in Figure 4A and the final signal shown in Figure 4B are similar. Contrary to the stage-2 results, there is not a large increase in signal after the initial time step, and the pattern of the CSEM response from this stage is asymmetric about the wellbore. Additionally, the largest CSEM response is found at greater distance from the well than the largest responses observed during the stage-2 operations. The great distance at which the largest CSEM response occurs indicates that a larger hydraulic fracture half-length was created in this stage relative to the previous one.

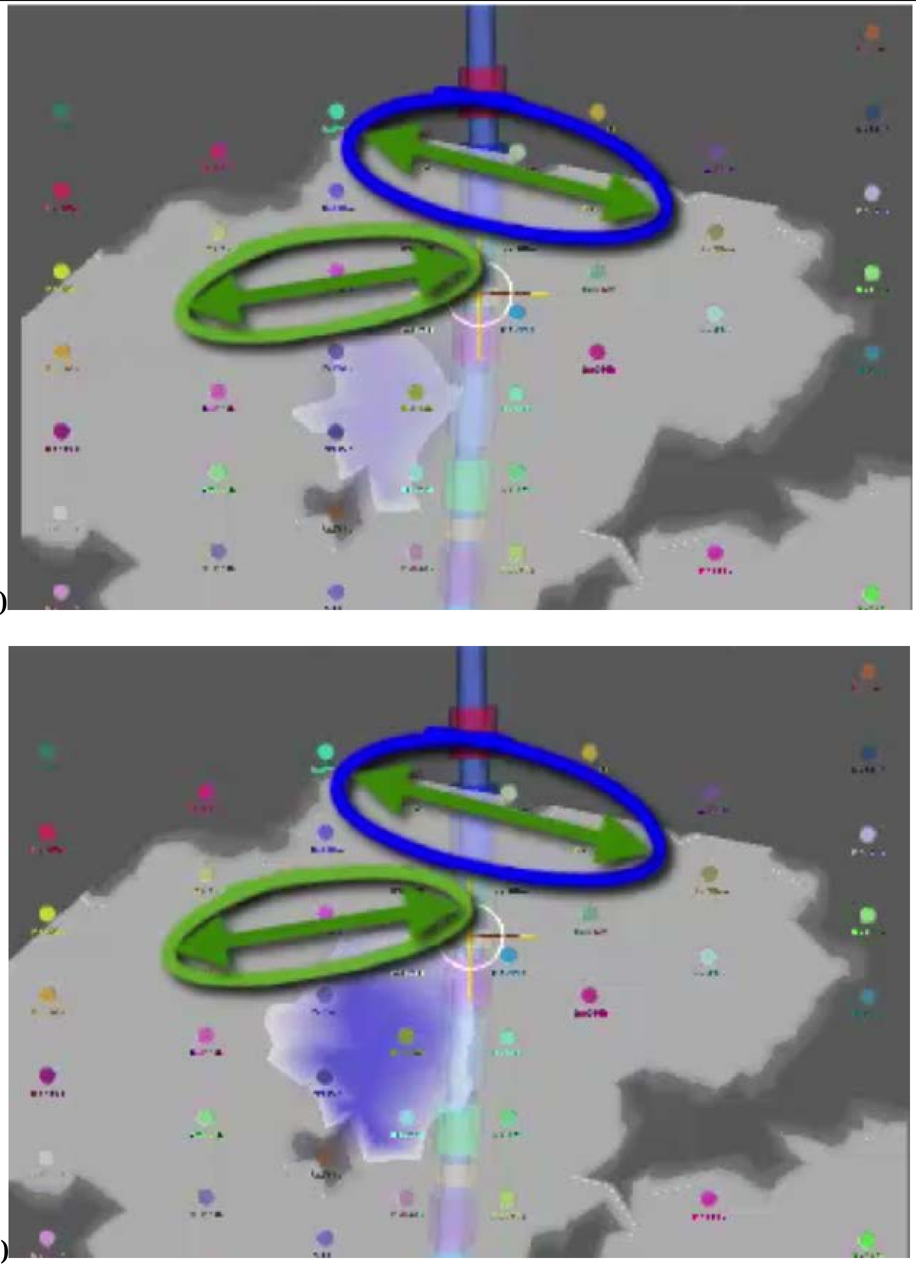
A)
B)

Figure 5: Stage 4 displaying the A) Initial frac signal B) Final frac signal.

The Stage-4 operation is different from previous stages in that it had fewer perforation clusters and was confined to a smaller length along the lateral. The CSEM responses are shown in Figures 5A and 5B with similar results to the stage-3 operation. An appreciable CSEM signal appears on only one side of the wellbore. Additionally, the fracture half-length is similar to that created during the stage-2 operation.

Case Study 2: Delaware Basin / Northwest Shelf

This case study is atypical of our past hydraulic fracture monitoring experience in unconventional settings in that the fluid injection wellbore is vertical. Consequently, the transmitter and receivers are placed on and/or close to the well pad, as shown in Figure 6. The main difficulty from a CSEM monitoring standpoint about this configuration is the large amount of electromagnetic noise that is generated by oilfield infrastructure and associated operations on the pad. Unfortunately, the noise level at some of the receivers proved excessively high and information acquired by these receivers has been removed from the dataset. Fortunately, the data from the remaining receivers are useful. The response at these receivers from hydraulic fracture fluid movement is manifest as change of CSEM signal over time that is distinguishable from the environmental noise. Another aspect of this case study is the target structure. The target structure in this case is a carbonate with inherent natural fractures. The natural fractures induces a larger fracture network. For the interpretation of these data, the signal was represented across a large frequency band, with each group of frequencies responding to a different aspect of the fluid movement. Instead of summing across the entire active bandwidth, for each stage we show for the 2D display only the most active frequency bands . Also, since the stages occurred at different depths, the active frequency bands were different at each stage. This is why different stages generate diagnostic CSEM responses over different frequency bands. The results from two stages are now discussed.

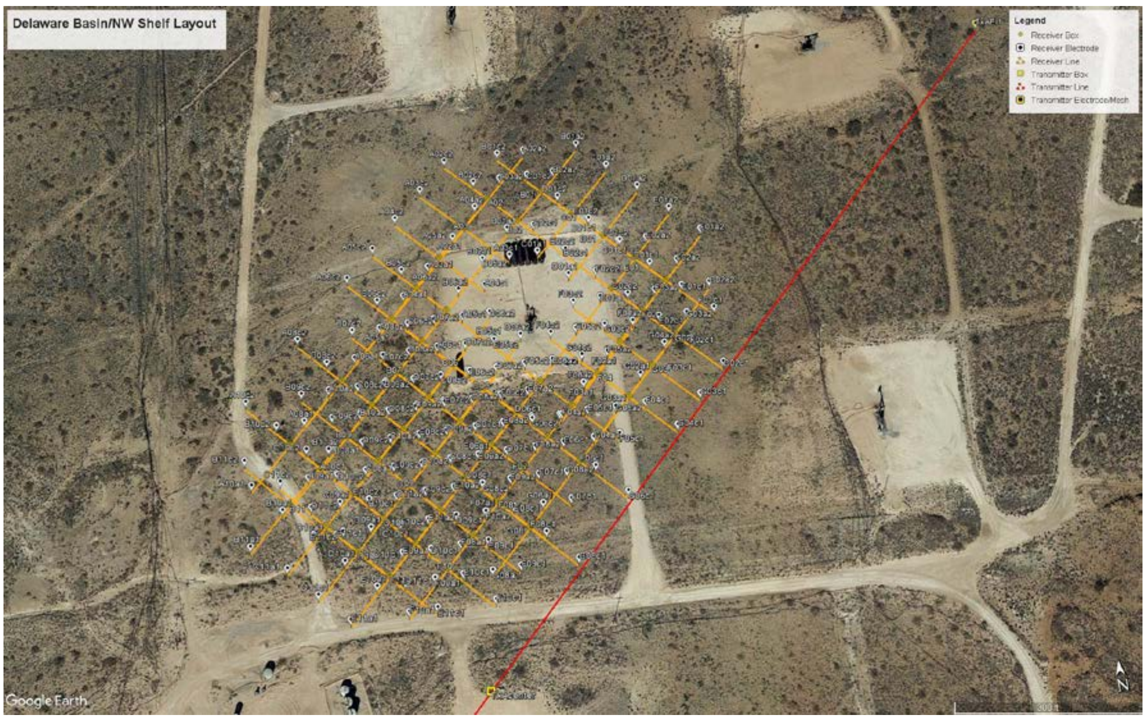

Figure 6. Delaware Basin / NW Shelf Layout

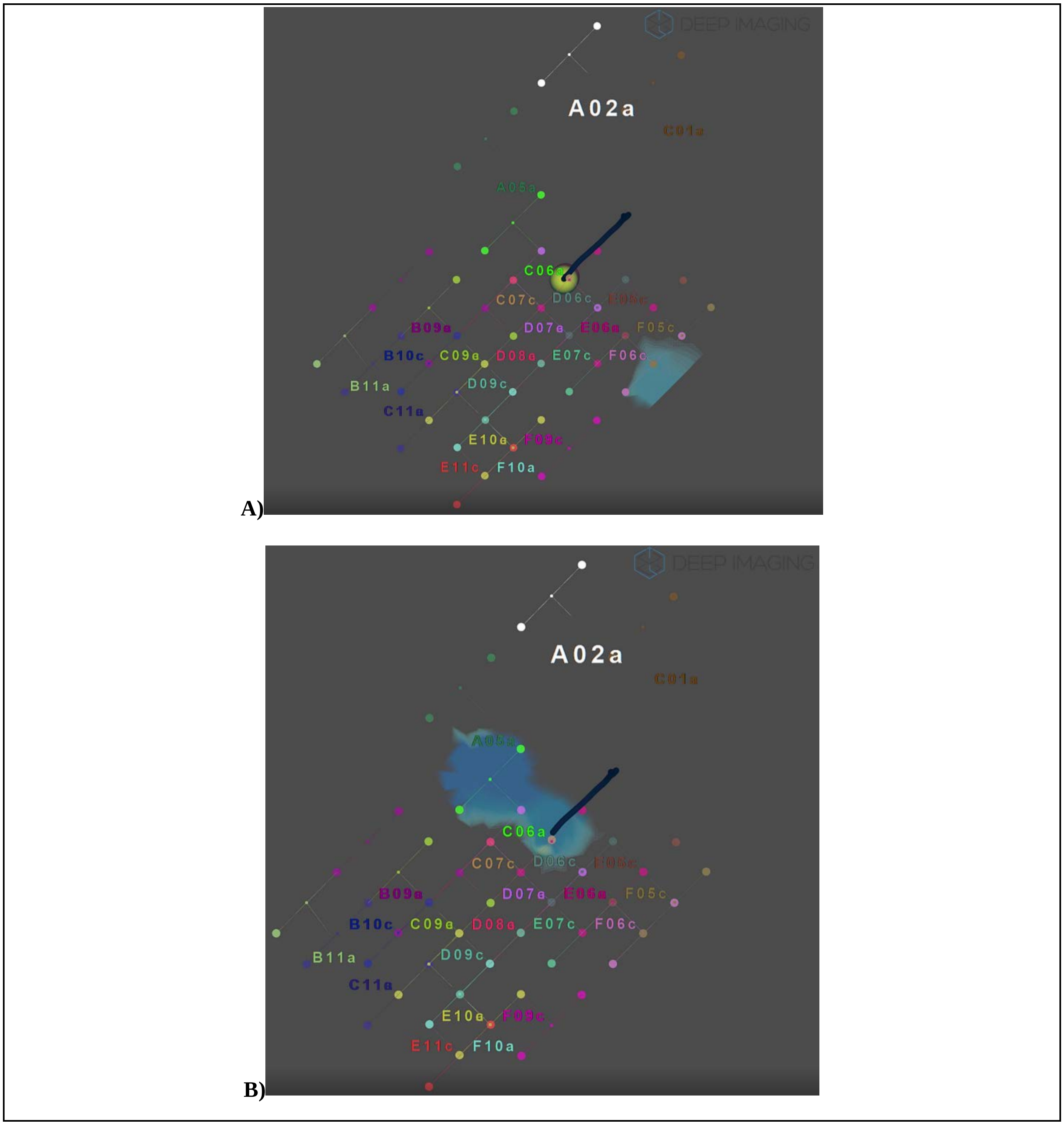

Figure 7 Stage 1 A) pre-frac data. B) initial frac data.

The CSEM signals from stage-1 operations are shown in Figures 7 and 8. The signal amplitudes from the frequency range 29-30 Hz have been summed to produce the aggregate signal shown in the figures. Figure 7A shows the background CSEM response prior to the beginning of the frac operation. The signal at this time is most likely due to the operations noise from the pad. As shown in Figures 7B, 8A and 8B, as the stage progresses, this signal disappears. Figure 7B shows that the zone of greatest response appears initially to the NW of the wellbore. This direction is aligned against the expected stress-direction pattern that was provided to us by the client. In Figure 8A, which corresponds to ~10 minutes from the beginning of the frac operation, the signal builds to the west. The final snapshot in Figure 8B shows the CSEM-response as an indicator of the culminating fluid and proppant distribution.

Note that the lack of usable receiver data to the NE of the wellbore, and on the pad itself, prevents a reliable interpretation of the progress of injected fluid in that direction.

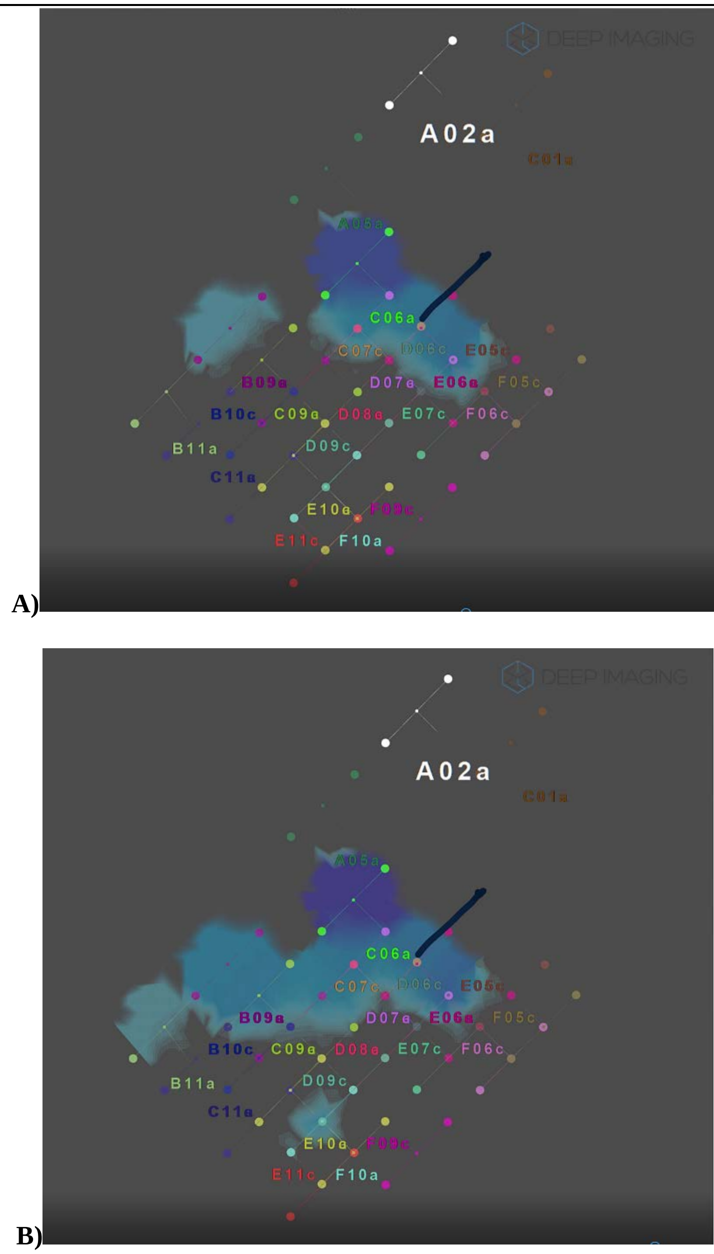

Figure 8: Stage 1 A) mid frac data. B) final frac data.

For the deeper stage-2 operation at this site, CSEM signals were summed in the lower frequency range 11-12 Hz and the results are shown in Figure 9. For operations at this stage, as in the previous stage, data from some of the receivers located near the pad were removed due to excessive noise levels. Figure 9A shows the regions where the largest CSEM signals are observed before the end of the hydraulic fracture. Figure 9B shows a post-frac image wherein it is noted the signal has dropped significantly. This result is interpreted as poor proppant placement into the formation around the wellbore.

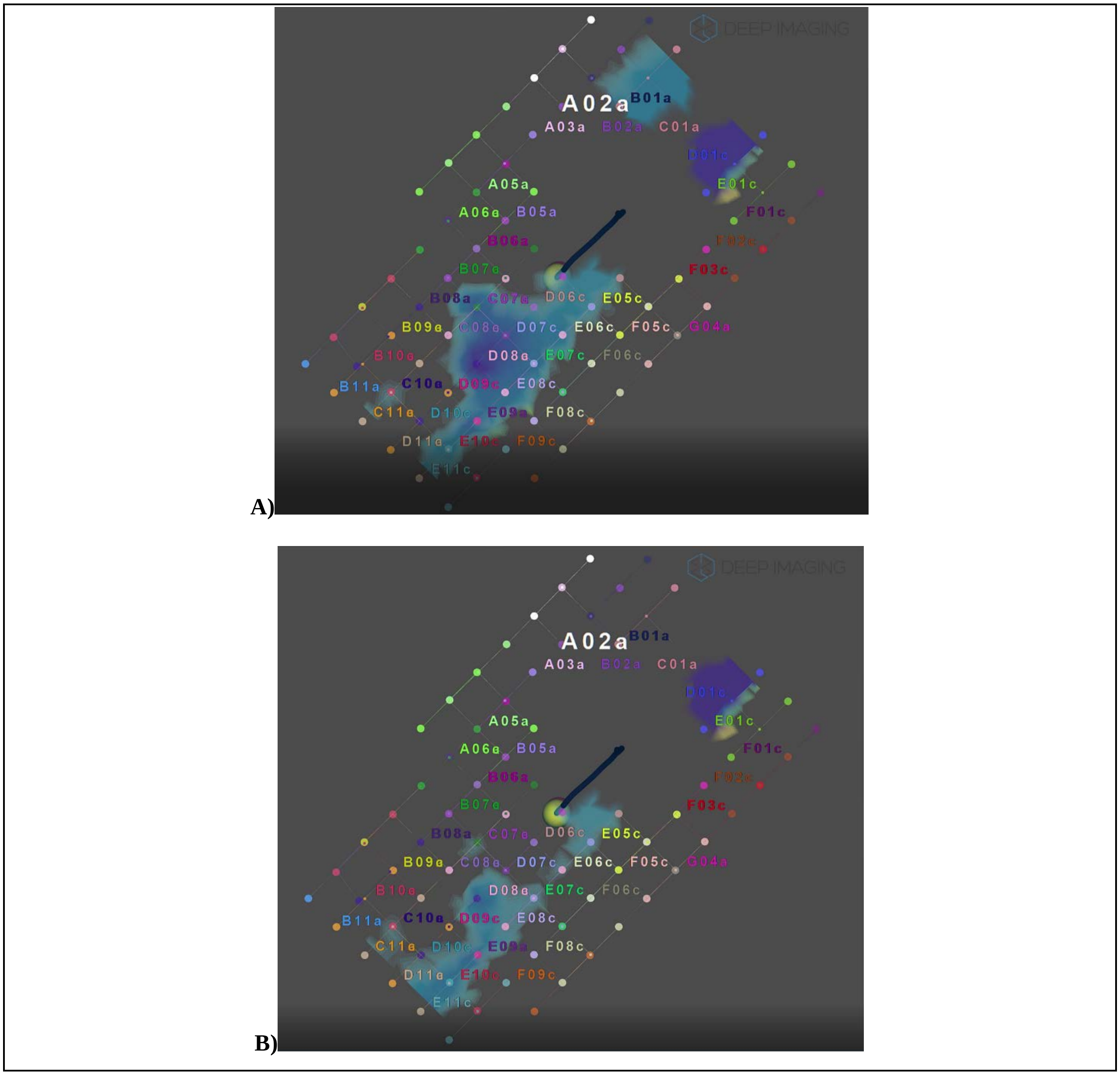

Figure 9: Stage 2 A) final stage data. B) post-stage data

Conclusions

In this paper two case studies are presented that display the effectiveness of a CSEM land-based geophysical system when it is used for hydraulic fracture monitoring. A key assumption is made that the observed temporal changes in the CSEM response are caused solely by corresponding changes in subsurface electrical conductivity induced by the movement of conductive fracture fluid. Future work aims to rigorously test this assumption. In the first case study involving a horizontal wellbore, the CSEM monitoring indicated frac fluid movement, fracture extent and asymmetry, as well as the azimuth of the principal fluid pathways. These properties can enhance future decisionmaking by the well development team such as well-spacing and repeat fracturing. The second case study, involving a vertical wellbore, introduced new challenges such as environmental electromagnetic noise from the pad-site oilfield activities. Nevertheless, an indication of frac fluid movement, its extent, as well as the quality of proppant placement, were attained. Future modifications to the system to mitigate pad noise will be investigated. For both case studies, the advantages of the sensitivity of a CSEM land-based geophysical system to the movement of hydraulic fracture fluid were demonstrated.

References

1) Hickey, M. S., Treviño III, S., & Everett, M. E. (2015). Detection and Characterization of the Injection of Hydraulic Fracturing Fluid using Ground-Based Controlled-Source Electromagnetics. In *SEG Technical Program Expanded Abstracts 2015* (pp. 1039-1043). Society of Exploration Geophysicists.

2) Hickey, M. S., Treviño III, S., & Everett, M. E. (2015, July). Monitoring and Imaging the Dynamics and Extent of Hydraulic Fracturing Fluid Movement Using Ground-Based Electromagnetics, with Application to the Eagle Ford Shale. In *Unconventional Resources Technology Conference, San Antonio, Texas, 20-22 July 2015* (pp. 2417-2429). Society of Exploration Geophysicists, American Association of Petroleum Geologists, Society of Petroleum Engineers.

3) Badea, E. A., Everett, M. E., Newman, G. A., & Biro, O. (2001). Finite-element analysis of controlled-source electromagnetic induction using Coulomb-gauged potentials. *Geophysics*, *66*(3), 786-799.

4) Patzer, C., Tietze, K., & Ritter, O. (2017). Steel-cased wells in 3-D controlled source EM modelling. *Geophysical Journal International*, *209*(2), 813-826.

5) Puzyrev, V., Vilamajo, E., Queralt, P., Ledo, J., & Marcuello, A. Three-Dimensional Modeling of the Casing Effect in Onshore Controlled-Source Electromagnetic Surveys. *Surveys in Geophysics*, 1-19.